Rafal Ploski ORCID iD: 0000-0001-6286-5526

Holger Prokisch ORCID iD: 0000-0003-2379-6286

Title

Expanding the clinical and genetic spectrum of FDXR deficiency by functional validation of variants of uncertain significance

Authors

Sarah L. Stenton[1,2], Dorota Piekutowska-Abramczuk[3], Lea Kulterer[1,2], Robert Kopajtich[1,2], Kristl G. Claeys[4,5], Elżbieta Ciara[3], Johannes Eisen[7], Rafał Płoski[8], Ewa Pronicka[3], Katarzyna Malczyk[6], Matias Wagner[1,2], Saskia B. Wortmann[1,2,9,10], Holger Prokisch[1,2]

1. Institute of Human Genetics, Technische Universität München, Munich, Germany.
2. Institute of Neurogenomics, Helmholtz Zentrum München, Munich, Germany.
3. Department of Medical Genetics, Children's Memorial Health Institute (CMHI) Warsaw, Poland.
4. Department of Neurology, University Hospitals Leuven, Leuven, Belgium.
5. Laboratory for Muscle Diseases and Neuropathies, Department of Neurosciences, KU Leuven, Leuven, Belgium.
6. Department of Diagnostic Imaging, Children's Memorial Health Institute (CMHI) Warsaw, Poland.

This article has been accepted for publication and undergone full peer review but has not been through the copyediting, typesetting, pagination and proofreading process, which may lead to differences between this version and the Version of Record. Please cite this article as doi: 10.1002/humu.24160.

7. Klinikum Frankfurt Höchst, Frankfurt, Germany.

8. Department of Medical Genetics, Medical University of Warsaw, Poland

9. Department of Pediatrics, Salzburger Landeskliniken and Paracelsus Medical University, Salzburg, Austria.

10. Radboud Centre for Mitochondrial Diseases (RCMM), Amalia Children's Hospital, Radboudumc, Nijmegen, The Netherlands.

Corresponding author

Dr. Holger Prokisch

Institut für Humangenetik, Klinikum rechts der Isar, Technische Universität München

Trogerstraße 32, 81675 München, Germany

E-mail: prokisch@helmholtz-muenchen.de

Number: +49 89 3187 2890

Conflict of interest statement

All authors declare no conflict of interest.

Keywords

Mitochondrial disease, Variant of uncertain significance, Functional validation, Phenotype, Leigh syndrome

Abstract

Ferrodoxin reductase (FDXR) deficiency is a mitochondrial disease described in recent years primarily in association with optic atrophy, acoustic neuropathy, and developmental delays. Here, we identified seven unpublished patients with FDXR deficiency belonging to six independent families. These patients show a broad clinical spectrum ranging from Leigh syndrome with early demise and severe infantile-onset encephalopathy, to milder movement disorders. In total nine individual pathogenic variants, of which seven were novel, were identified in *FDXR* using whole exome sequencing in suspected mitochondrial disease patients. Over 80% of these variants are missense, a challenging variant class in which to determine pathogenic consequence, especially in the setting of non-specific phenotypes and in the absence of a reliable biomarker, necessitating functional validation. Here we implement an *Arh1*-null yeast model to confirm the pathogenicity of variants of uncertain significance (VUS) in *FDXR*, bypassing the requirement for patient-derived material.

Introduction

FDXR encodes the mitochondrial membrane-associated ferredoxin reductase, an enzyme essential for the biosynthesis of iron-sulfur (Fe-S) clusters, integral to electron transport in mitochondrial respiration (Ewen et al., 2011, Jung et al., 1999, Stehling et al., 2014, Beilschmidt et al., 2014, Johnson et al., 2005). Defects in this protein thereby lead to dysregulated iron homeostasis, abnormal iron uptake and iron overload in mitochondria, resulting in major oxidative stress and mitochondrial dysfunction (Paul et al., 2017, Hwang et al., 2001). FDXR deficiency (MIM# 617717) is one of more than 10 disorders of lipoic acid and iron-sulfur protein metabolism (Ferreira et al., 2019).

Since the initial description in 2017, 27 patients have been reported with FDXR deficiency (Paul et al., 2017, Peng et al., 2017, Slone et al., 2018). The majority of these patients are unified by presentation with optic atrophy and acoustic neuropathy. In patients with an early manifestation of disease, developmental regression often on the background of developmental delay is a common feature. A lesser number of patients present with the broad neurological signs of mitochondriopathy, such as hypotonia, spasticity, ataxia, movement disorders, and seizures. In keeping with other mitochondrial diseases, clinical deterioration is often associated with infection. Abnormalities on brain MRI are reported in both the white and grey matter (Peng et al., 2017). Collectively, published studies describe 24 unique pathogenic *FDXR* variants. In a proof of principle approach, a limited number of variants were validated in an *Arh1*-null yeast model developed by Paul and colleagues (Paul et al., 2017). The yeast mitochondrial *Arh1* shares 35% identity with the human *FDXR*, and is confirmed to be the functional orthologue (Manzella et al., 1998). In the absence of *Arh1*, lethality results. The inability to rescue the *Arh1*-null model by overexpression of mutant *FDXR* can therefore be utilized in functional validation of variants of uncertain significance (VUS) in *FDXR*, negating the need for patient material.

Herein, we report the results of the clinical and genetic findings in seven patients from six individual families harboring biallelic variants in *FDXR*, expanding the phenotypic and mutational spectrum of FDXR deficiency, and provide estimates of phenotype frequency in this heterogenous disease based on the collective 34 cases described to date. Moreover, we provide functional validation for seven novel VUS in *FDXR* using the *Arh1*-null yeast model.

Material and methods

Patient cohort and clinical examination

Patients harboring biallelic VUS in *FDXR* were identified via collaboration using the GeneMatcher database (www.genematcher.org) (Sobreira et al., 2014). Genetic and clinical patient data were collated from centers across Germany and Poland. This resulted in the collection of seven individuals from six families. Each patient was investigated by whole exome sequencing (WES) by their respective center as described by Kremer at al., 2017 and Pronicka et al., 2016. DNA was collected from available family members for confirmation of variant segregation by PCR and Sanger sequencing using standard procedures, primers available on request (**Figure 1A**). All patients or their legal guardian(s) gave consent approved by their respective local research and ethical boards or dependent on the local regulatory bodies.

Variant pathogenicity assessment

All published and novel variants were annotated on the transcript (NM_024417) and protein (NP_077728) level. The possible effects of the variants were assessed by the computational *in silico* tools, CADD (https://cadd.gs.washington.edu; Rentzsch et al., 2019), SIFT (http://sift.jvic.org; Kumar, Henikoff & Ng, 2009), and PolyPhen (http://genetics.bwh.harvard.edu/pph2/; Adzhubei et al., 2010). The variants were classified according to the standards and guidelines provided by the American College of Medical Genetics and Genomics (ACMG) (Richards et al., 2015).

Functional validation of variant pathogenicity in the *Arh1*-null yeast model

We employed the *Arh1*-null yeast model as previously described (Paul et al., 2017) to functionally validate VUS in *FDXR*. In brief, plasmids containing wild-type (wt) or mutant-*FDXR* were generated by site directed mutagenesis. 5-FOA treatment was utilized to eliminate the plasmid encoding the yeast *Arh1*, allowing evaluation of the growth capability of the *Arh1*-null cells expressing wild-type *FDXR* (wt) and the mutated *FDXR* forms. Cells were spotted onto YPD (yeast extract-peptone-dextrose) or YPG (yeast extract-peptone-glycerol) plates. Drop dilution growth tests were performed at 1/5 dilution steps (initially with 2,000,000 seeded cells), and plates were incubated for 3 days at either 30°C or 35°C. Four conditions were selected for the stepwise assessment of variant severity. Condition (1) YPD, 30°C, (2) YPD, 35°C, (3) YPG, 30°C and (4) YPG, 35°C. The YPD medium is fermentable and permits glycolysis to generate cellular ATP. The YPG medium is non-fermentable and requires oxidative phosphorylation (OXPHOS) in the mitochondrial to generate cellular ATP. The corresponding empty plasmid (-) and p.Arg242Trp variant were included as positive controls. The p.Arg123Gln (wt) variant was used as a negative control, as a commonly occurring polymorphism in the gnomAD database (allele frequency 20.1%). The severity of the yeast defect was categorized into a 5-tier system (1, most severe, 5, least severe) based on the growth condition and dilution.

Calculation of clinical severity by a modified NPMDS score

The Newcastle Paediatric Mitochondrial Disease Scale (NPMDS) (Phoenix et al., 2006) was modified to provide an objective measure of disease severity comparable between patients and pediatric age groups, given the wide array of associated symptoms (**Supp. Table S1**). This resulted in a multi-systemic scoring system

encompassing 20 phenotypes, each with a possible score of 0 (normal), 1 (mild), 2 (moderate), and 3 (severe), and one phenotype category "Developmental" with a possible score of 0 (normal), 1-2 (isolated motor, speech, language, or hearing delay with or without developmental progression), 5-6 (global developmental delay with or without progression), and 7 (developmental regression). Utilizing patient case reports a score was calculated for all 27 published and seven newly described patients. Correlation of the clinical severity score with the severity of the growth defect in the yeast was analyzed by computing the Pearson correlation coefficient using R version 1.1.423. Additional published cases were included in this analysis when carrying variants tested in our model.

Results

The mutational spectrum of FDXR deficiency

Here, we report seven individuals from six families harboring nine different biallelic variants in *FDXR* (**Figure 1A**). Where parental DNA samples were available, the variants were confirmed to be inherited by biparental transmission. In Family 1, parental DNA was not available. However, reduction in the FDXR protein in the patient-derived fibroblast cell line on Western blot to 27.8% of control provided strong evidence for the compound heterozygous nature of the variants.". In Family 4, one variant allele was paternally-inherited and the second variant arose *de novo*. The variant positions are highly conserved across species (**Figure 1C**).

Considering all reported cases to date, the mutational spectrum of FDXR deficiency spans 31 unique variants (**Table 1**), distributed throughout the entire gene and protein structure (**Figure 1C**). Of these variants 24 were previously reported and seven are

novel to this study. The majority of variants are missense (25, 80.6%), with a lesser number of nonsense (3, 9.7%), indel (2, 6.5%), and start-loss (1, 3.2%) variants reported. There is no report of biallelic loss-of-function variation, indicating the gene to be essential. The allele frequency of all reported variants in gnomAD is <0.1% and no homozygous carriers are documented (**Table 1**). The CADD score was invariably greater than 20 (range 21.4 to 44), indicating this to be a suitable threshold for consideration of an *FDXR* variant as pathogenic. However, on inspection of the gnomAD database of presumably healthy individuals, of 14 homozygous *FDXR* variants reported (seven rare, allele frequency <0.1%, seven common, allele frequency >0.1%), five have a CADD score greater than 20 and can be confidently assumed not to cause overt disease (**Figure 1C**). The SIFT and PolyPhen *in-silico* pathogenicity prediction tools provide supporting evidence in all of the variants in the patients (**Table 1**). Calculation of the ACMG criteria deemed all missense variants, with the exception of p.Leu215Val and p.Gly437Cys (both "Likely pathogenic"), to be "Variants of uncertain significance" (VUS) without the addition of functional evidence (**Table 1**).

The clinical spectrum of FDXR deficiency

A summary of the clinical features of the newly described patients in this study are displayed in **Table 2**. Optic atrophy and hearing impairment are reported in five and four patients (71.4% and 57.1%), respectively. These previously commonly reported FDXR deficiency features were seen in association with a range of muscular, neurological, and ophthalmological phenotypes spanning myopathy, hypotonia, developmental regression, developmental delay, seizures, microcephaly, movement disorder, ataxia, spasticity, ptosis, ophthalmoplegia, and nystagmus. The most

severely affected patients presented with the infantile-onset neurological phenotypes of Leigh syndrome (Subject 2) and of familial encephalopathy with delayed myelination (Subject 4).

Focusing on these severe presentations, Subject 2 presented with the triad of clinical features indicating a diagnosis of Leigh syndrome: progressive neurological disease with motor and intellectual developmental delay, signs and symptoms of basal ganglia disease, and raised lactate in the cerebrospinal fluid (CSF) (Rahman et a., 1996). To our knowledge this is the first patient presenting with Leigh syndrome caused by FDXR deficiency. In brief, this male patient was born to nonconsanguineous parents following an uncomplicated anti-, peri-, and postnatal course. His development was unremarkable until the age of 7 months, when he experienced onset of an intermittent horizontal nystagmus and motor developmental regression. At this time, his MRI brain revealed optic atrophy but was otherwise unremarkable. A later MRI investigation at 10 months however, revealed diffusion weighted imaging (DWI) changes bilaterally in the pallidal globe and thalami suggestive of Leigh syndrome (**Figure 2A**). Moreover, lactate was measured to be elevated in the cerebrospinal fluid (CSF, 2.4 mmol/L, normal range 1.2-2.1 mmol/L). At the age of 11 months he presented with high fevers and a raised CRP (30 mg/L, normal range <5 mg/L) with no clear focus of infection. He subsequently succumbed to epileptic seizures, loss of consciousness, and loss of brain stem reflexes including respiratory drive and blood pressure regulation. Due to the very rapid deterioration and the MRI findings suggestive of Leigh syndrome, treatment was withdrawn and the patient immediately passed away.

Subject 4 presented with infantile-onset progressive encephalopathy with delayed myelination. In brief, this male patient was born to nonconsanguineous parents. He has a healthy older sister and an older brother whom died at the age of 6 months of a similar disease course as the index patient. The first symptoms were noted at the age of 2 months, of global developmental delay, axial weakness, poor head control, muscle hypotonia, no response to auditory stimuli, and absence of fixing and following of objects. At 4.5 months of age, bilateral nuclear cataracts and severe hearing loss were diagnosed. From 7 months of age disease progression was noted with poor weight gain, involuntary movement, inability to sit or to stabilize the head, and limb spasticity. Physical examination revealed microcephaly, slight facial dysmorphism with frontal bossing, a high-arched palate, areflexia, and incomplete knee extension. Laboratory tests demonstrated a normal lactate. A radiologic skeletal survey reported delayed bone age. Muscle biopsy demonstrated nonspecific variability of muscle fiber size with no signs of neurogenic damage. The spectrophotometry of mitochondrial respiratory chain complex (RCC) enzyme activity measured a combined RCC defect (CI, II, and CIV), in keeping with the variable RCC defects described previously in FDXR deficiency, as well as for other disorder of iron-sulfur (Fe-S) cluster biosynthesis (Coelho et al., 2019, Rötig et al., 1997). Magnetic resonance imaging (MRI) of the brain at the age of 5 months demonstrated delayed myelination (**Figure 2B**) in keeping with that expected of a child aged younger than 3 months, and hypoplasia or atrophy of the optic chiasm and mega cisterna magna (**Figure 2C**). Delayed myelination was confirmed in follow-up MRI scan at the age of 13.5 months (**Figure 2D**) in keeping with that expected of a child aged younger than 8 months, in addition to slight vermis atrophy, decreased volume of thalami and of the white matter of occipital lobes, and slightly enlarged

frontal cerebral spaces. Both MRI scans revealed signal abnormalities in lateral aspects of thalami on the T2 weighted images (**Figure 2D**), without progression, and with no abnormal restriction of diffusion.

The complete phenotypic spectrum of FDXR deficiency, as reported in the seven cases described here and the 27 previously reported cases, is displayed in **Supp. Table S2**. These phenotypes primarily span the neurological, muscular, and ophthalmological systems. The most frequently reported phenotypes are optic atrophy (29, 85.3%), visual impairment (23, 67.6%), neurodevelopmental delays (22, 64.7%, encompassing global, motor, and speech and language delay), hearing impairment (16, 47.1%), developmental regression (16, 47.1%, of which 93.8% arose on the background of neurodevelopmental delay), and hypotonia (15, 44.1%). With the addition of patients from our study, supporting evidence is provided for the association of delayed myelination, dystonia, ophthalmoplegia, and cataracts with FDXR deficiency, previously reported in single cases only. Ptosis and type I diabetes mellitus, phenotypes known to be associated with other disorders of iron-sulfur protein metabolism such as Friedreich ataxia (Cnop et al., 2013, Filla et al., 1990), are described here for the first time in individuals with FDXR deficiency. Interestingly, despite complexes I, II, and III containing iron-sulfur (Fe-S) clusters, defects in the mitochondrial respiratory chain complex (RCC) enzymes are reported in just 6 of 12 investigated patients (50.0%), with complex I most commonly defective (5/6, 83.3%), followed by complex III and IV (4/6, 66.7% and 3/6, 50%, respectively).

Functional validation of VUS in the *Arh1*-null yeast model

The *FDXR* variants of uncertain significance (VUS) from each patient were functionally validated in the *Arh1*-null yeast model (**Figure 3**). The conditions

progressed from provision of a fermentable substrate (YPD) at 30°C and 35°C to a non-fermentable substrate (YPG) at 30°C and 35°C, obliging the yeast to respire by mitochondrial oxidative phosphorylation (OXPHOS) and progressively stressing the cells. The results indicated that each of the novel variants disrupt the function of FDXR to a varying degree within a 5-tier system (**see Methods**), thereby confirming the pathogenicity of all tested variants.

Determining clinical severity by means of functional validation

The severity of the clinical phenotype, as calculated by a modified NPMDS (**see Methods**), ranged from 3 to 27 (median 14) in our patients, representing mild to severe multi-systemic disease. This breadth of clinical severity is in-keeping with the previously reported cases (range 2 to 24, median 14), and is inclusive of a number of more severely affected patients, Subject 2 with Leigh syndrome and Subject 4 with progressive encephalopathy and delayed myelination, as described. Across all reported cases, 18 variants were inherited in a homozygous fashion. Of these 18 variants, three variants presented in more than one patient; p.Arg306Cys (n=4), p.Asp368Asn (n=2), and p.Arg386Trp (n=8), allowing comparison of the phenotype. Patients carrying the same variant demonstrated marked similarity in clinical severity score, with p.Arg306Cys resulting in the mildest phenotype (mean 3.6, s.d. 1.52), p.Asp368Asn resulting in the most severe phenotype (mean 21.5, s.d. 0.71), and p.Arg386Trp in a moderately severe phenotype (mean 14.3, s.d. 3.16) (**Supp. Figure S1**). The clinical severity score was not found to correlate with the severity of the growth defect in the yeast model (**Supp. Figure S2**), indicating that this functional validation assay is unable to predict the resultant clinical severity. Concerning mitochondrial RCC enzyme defects, there was no difference in NPMDS score

between those with (n=6, mean 14.2, s.d. 8.93) and without (n=6, mean 17.5, s.d. 5.09) an OXPHOS defect on muscle biopsy (p-value 0.95, two-sided Student's t-test), where investigated (**Supp. Figure S3**).

Discussion

FDXR deficiency is an autosomal recessive mitochondrial disease and disorder of iron-sulfur (Fe-S) cluster biosynthesis, with an estimated lifetime risk of 0.11 per 100,000 (95% CI, 0.08-0.14), deeming it amongst the 50 mitochondrial disease of highest prevalence (Tan et al., 2020). Reflecting this, we collate the genetic and phenotypic data of over 30 patients with FDXR deficiency. As an essential gene, variation in *FDXR* presents with a phenotypic spectrum from relatively benign disorders to severe multi-systemic infantile-onset disease with early lethal course, and to date, no patient is reported to carry two loss-of-function variants expected to be incompatible with life. Akin to the other disorders of iron-sulfur protein metabolism, such as Friedreich ataxia, here we report FDXR deficiency in association with neuropathy (optic atrophy, acoustic neuropathy), ataxia, and nystagmus, in addition to the newly FDXR deficiency associated symptoms of ptosis and type I diabetes mellitus in isolated cases. Interestingly, other key features of Friedreich ataxia (MIM# 229300), such as hypertrophic cardiomyopathy, are not observed in these patients. Moreover, though we recapitulate the previously reported commonly occurring phenotypes, such as optic atrophy, acoustic neuropathy, and developmental delays with regression, we also report the first case of FDXR deficiency meeting the diagnostic criteria for Leigh syndrome in accordance with Rahman et al., 1996. This patient presented with the triad of developmental regression, bilateral basal ganglia changes, and elevated CSF lactate, in addition to features frequent to FDXR

deficiency, such as optic atrophy. Moreover, we provide further supporting evidence for the association of delayed myelination, dystonia, ophthalmoplegia, and cataracts with FDXR deficiency. These phenotypes were previously only reported in isolated cases (Paul et al., 2017, Peng et al., 2017, Slone et al., 2018). The demonstration of further patients with these phenotypes and a common molecular cause increases the evidence for their link to the underlying genetic diagnosis and indicates that they are less likely to be sporadic unrelated occurrences. This is important for genetic counselling. In terms of counselling families on disease severity, we report patients carrying the same genetic variant to demonstrate similarity in clinical severity, exemplified by the homozygous p.Arg306Cys carriers invariably expressing a mild phenotype and the homozygous p.Asp368Asn carriers invariably expressing a severe phenotype. However, such pattern recognition requires the collection of multiple patients harboring the same variant(s). In patients carrying unique variants, it is challenging given the absence of correlation between the severity of the growth defect in the yeast model, to predict clinical severity. These data should not therefore be relied upon to direct genetic counselling.

With no specific biomarker for FDXR deficiency, and no consistent defect in OXPHOS respiratory chain complex enzymes on muscle biopsy, an alternative assay is necessitated in the clinical work-up of the patient. Moreover, given the large number of variants of relative high allele frequency, the non-specificity of the phenotypes involved in FDXR deficiency, and the vast majority of newly discovered VUS being missense (80.6%), determination of pathogenicity is challenging and functional validation becomes essential. It becomes especially difficult to differentiate between these alleles when only a small amount of residual protein is needed to maintain function. This is true not only of FDXR deficiency, but of almost all

mitochondrial diseases. Amongst the mitochondrial disease genes, over two thirds have a yeast ortholog, making this a useful assay, negating the need for patient derived materials (Stenton and Prokisch 2020). Moreover, yeast models offer ease in genetic manipulation and rapid growth.

Here, we demonstrate the utility of an *Arh1*-null yeast model in validation of seven novel and three previously described pathogenic *FDXR* variants. The pathogenicity of these variants was revealed by stepwise changes to growth conditions in order to sequentially stress the *Arh1*-null yeast cells expressing the mutant FDXR protein. This may have limitations, as pathogenicity arguably becomes questionable in the most unfavorable of these conditions, and the results must be considered with caution. When taken beyond the conditions selected here, we may even observe differences between wild-type and common polymorphisms. For this reason, we chose to include a common polymorphism in the analysis as a negative control, p.Arg123Gln (allele frequency 20.1% in gnomAD). Interestingly, we did not find correlation between the severity of the growth defect in the yeast with the severity of the patient's clinical presentation. Though this indicates that the model does not have value is phenotype severity prediction, it does allow the model to be useful for confirmation of variant pathogenicity even in patients with a very subtle clinical phenotype.

Web resources

CADD: https://cadd.gs.washington.edu

SIFT: http://sift.jvic.org

PolyPhen: http://genetics.bwh.harvard.edu/pph2/

Acknowledgements

This study was supported by a German Federal Ministry of Education and Research (BMBF) grant to the German Network for Mitochondrial Disorders (mitoNET, 01GM1906D to H.P.), by the German BMBF and Horizon2020 through the E-Rare project GENOMIT (European Network for Mitochondrial Diseases, 01GM1920A to H.P.), the ERA PerMed project PerMiM (01KU2016A to H.P. and S.W.) and CMHI grants (S145/16 to D.P.).

Data Availability Statement

The variants described in the patients of this manuscript have been submitted to ClinVar. The data that support the findings of this study are available on request from the corresponding author. The data are not publicly available due to privacy or ethical restrictions.

References

Adzhubei, I. A., Schmidt, S., Peshkin, L., Ramensky, V. E., Gerasimova, A., Bork, P.,... & Sunyaev, S. R. (2010). A method and server for predicting damaging missense mutations. Nature methods, 7(4), 248-249.

Beilschmidt, L. K., & Puccio, H. M. (2014). Mammalian Fe–S cluster biogenesis and its implication in disease. Biochimie, 100, 48-60.

Cnop, M., Mulder, H., & Igoillo-Esteve, M. (2013). Diabetes in Friedreich ataxia. Journal of neurochemistry, 126, 94-102.

Coelho, M. P., Correia, J., Dias, A., Nogueira, C., Bandeira, A., Martins, E., & Vilarinho, L. (2019). Iron-sulfur cluster ISD11 deficiency (LYRM4 gene) presenting as cardiorespiratory arrest and 3-methylglutaconic aciduria. JIMD reports, 49(1), 11-16.

Ewen, K. M., Kleser, M., & Bernhardt, R. (2011). Adrenodoxin: the archetype of vertebrate-type [2Fe–2S] cluster ferredoxins. Biochimica et Biophysica Acta (BBA)-Proteins and Proteomics, 1814(1), 111-125.

Ferreira, C. R., van Karnebeek, C. D., Vockley, J., & Blau, N. (2019). A proposed nosology of inborn errors of metabolism. Genetics in Medicine, 21(1), 102-106.

Filla, A., DeMichele, G., Caruso, G., Marconi, R., & Campanella, G. (1990). Genetic data and natural history of Friedreich's disease: a study of 80 Italian patients. Journal of neurology, 237(6), 345-351.

Hwang, P. M., Bunz, F., Yu, J., Rago, C., Chan, T. A., Murphy, M. P.,... & Vogelstein, B. (2001). Ferredoxin reductase affects p53-dependent, 5-fluorouracil–induced apoptosis in colorectal cancer cells. Nature medicine, 7(10), 1111-1117.

Johnson, D. C., Dean, D. R., Smith, A. D., & Johnson, M. K. (2005). Structure, function, and formation of biological iron-sulfur clusters. Annu. Rev. Biochem., 74, 247-281.

Jung, Y. S., Gao-Sheridan, H. S., Christiansen, J., Dean, D. R., & Burgess, B. K. (1999). Purification and biophysical characterization of a new [2Fe-2S] ferredoxin from Azotobacter vinelandii, a putative [Fe-S] cluster assembly/repair protein. Journal of Biological Chemistry, 274(45), 32402-32410.

Kremer, L. S., Bader, D. M., Mertes, C., Kopajtich, R., Pichler, G., Iuso, A.,... & Koňaříková, E. (2017). Genetic diagnosis of Mendelian disorders via RNA sequencing. Nature communications, 8(1), 1-11.

Kumar, P., Henikoff, S., & Ng, P. C. (2009). Predicting the effects of coding non-synonymous variants on protein function using the SIFT algorithm. Nature protocols, 4(7), 1073.

Lin, D., Shi, Y. F., & Miller, W. L. (1990). Cloning and sequence of the human adrenodoxin reductase gene. Proceedings of the National Academy of Sciences, 87(21), 8516-8520.

Manzella, L., Barros, M. H., & Nobrega, F. G. (1998). ARH1 of Saccharomyces cerevisiae: a new essential gene that codes for a protein homologous to the human adrenodoxin reductase. Yeast, 14(9), 839-846.

Paul, A., Drecourt, A., Petit, F., Deguine, D. D., Vasnier, C., Oufadem, M.,... & Mahieu, L. (2017). FDXR mutations cause sensorial neuropathies and expand the spectrum of mitochondrial Fe-S-synthesis diseases. The American Journal of Human Genetics, 101(4), 630-637.

Peng, Y., Shinde, D. N., Valencia, C. A., Mo, J. S., Rosenfeld, J., Truitt Cho, M.,... & Brockhage, R. (2017). Biallelic mutations in the ferredoxin reductase gene cause novel mitochondriopathy with optic atrophy. Human molecular genetics, 26(24), 4937-4950.

Phoenix, C., Schaefer, A. M., Elson, J. L., Morava, E., Bugiani, M., Uziel, G.,... & McFarland, R. (2006). A scale to monitor progression and treatment of mitochondrial disease in children. Neuromuscular Disorders, 16(12), 814-820.

Pronicka, E., Piekutowska-Abramczuk, D., Ciara, E., Trubicka, J., Rokicki, D., Karkucińska-Więckowska, A.,... & Ploski, R. (2016). New perspective in diagnostics of mitochondrial disorders: two years' experience with whole-exome sequencing at a national paediatric centre. Journal of translational medicine, 14(1), 174.

Rahman, S., Blok, R. B., Dahl, H. H., Danks, D. M., Kirby, D. M., Chow, C. W.,... & Thorburn, D. R. (1996). Leigh syndrome: clinical features and biochemical and DNA abnormalities. Annals of Neurology: Official Journal of the American Neurological Association and the Child Neurology Society, 39(3), 343-351.

Rentzsch, P., Witten, D., Cooper, G. M., Shendure, J., & Kircher, M. (2019). CADD: predicting the deleteriousness of variants throughout the human genome. Nucleic acids research, 47(D1), D886-D894.

Rötig, A., de Lonlay, P., Chretien, D., Foury, F., Koenig, M., Sidi, D.,... & Rustin, P. (1997). Aconitase and mitochondrial iron–sulphur protein deficiency in Friedreich ataxia. Nature genetics, 17(2), 215-217.

Slone, J., Peng, Y., Chamberlin, A., Harris, B., Kaylor, J., McDonald, M. T.,... & Sellars, E. A. (2018). Biallelic mutations in FDXR cause neurodegeneration associated with inflammation. Journal of human genetics, 63(12), 1211-1222.

Sobreira, N., Schiettecatte, F., Valle, D., & Hamosh, A. (2015). GeneMatcher: a matching tool for connecting investigators with an interest in the same gene. Human

mutation, 36(10), 928-930.Stehling, O., Wilbrecht, C., & Lill, R. (2014). Mitochondrial iron–sulfur protein biogenesis and human disease. Biochimie, 100, 61-77.

Stenton, S. L., & Prokisch, H. (2020). Genetics of mitochondrial diseases: Identifying mutations to help diagnosis. EBioMedicine, 56, 102784.

Tan, J., Wagner, M., Stenton, S. L., Strom, T. M., Wortmann, S. B., Prokisch, H.,... & Klopstock, T. (2020). Lifetime risk of autosomal recessive mitochondrial disorders calculated from genetic databases. EBioMedicine, 54, 102730.

Figures

Figure 1. *FDXR* variants observed in this study and other published studies.

(A) Pedigrees of the investigated families. Variants in *FDXR* are reported according to the transcript annotation NM_024417. (+) indicates a wt allele; (-) indicates a mutant allele.

(B) Sequence alignment of ferredoxin proteins from various species. The arrows indicate the amino acid changes in the patients from this study. Emboldened amino acids are conserved.

(C) Schematic representation of the *FDXR* gene (NM_024417) and its predicted protein product (NP_077728) (Lin et al., 1990). Exons are represented with numbered boxes. The mitochondrial targeted sequence (MTS), and the locations of the NADP and FAD binding regions are shown in yellow, blue, and purple, respectively. The observed mutations are labelled, with previously reported pathogenic variants depicted in black, novel pathogenic variants reported in this study depicted in pink, and homozygous presumably benign variants from the gnomAD database depicted in green. The three-dimensional representation of the crystal structure of BOS ferredoxin reductase (PDB:1CJC) highlights the mutated residues from all reported patients (both reported and novel to this study, pink) and from healthy homozygous carriers in gnomAD

(green). The FAD and NADP binding regions are highlighted in blue and purple, respectively.

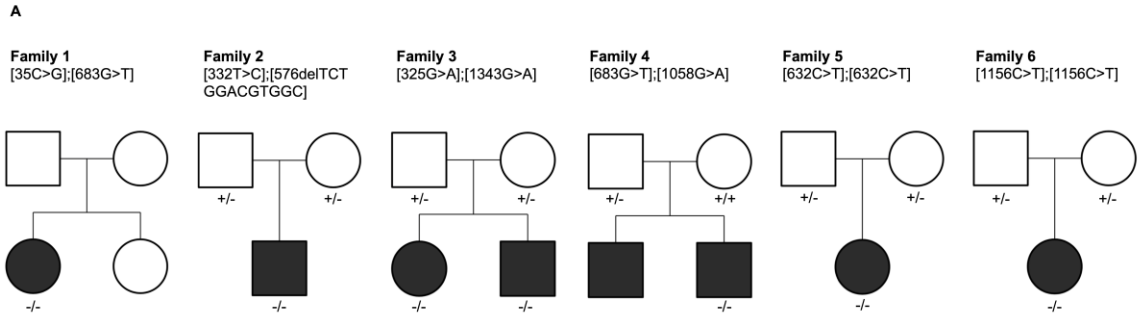

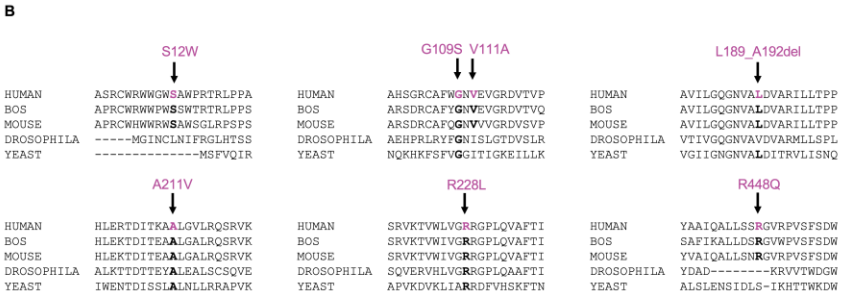

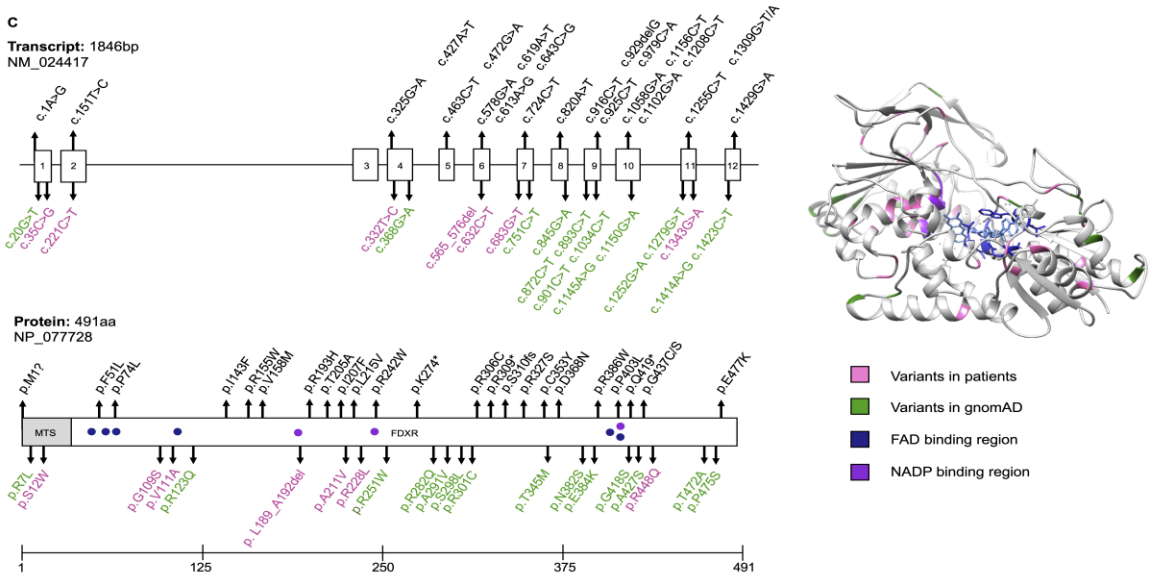

Figure 2. MRI images from the study patients with Leigh syndrome and delayed myelination.

(A) Diffusion weighted imaging (DWI) of the brain in Subject 2 at 10 months demonstrating changes bilaterally in the pallidal globe and thalami suggestive of Leigh syndrome.
(B) Axial T1-weighted MRI brain image shows lack of myelination of the optic radiation in Subject 4 at the age of 5 months.
(C) Sagittal T2-weighted MRI brain image also demonstrates hypoplasia or atrophy of the optic chiasm and mega cisterna magna in Subject 4 at the age of 5 months.
(D) Axial T2 weighted MRI brain of Subject 4 at the age of 13.5 months showing absence of myelination of the anterior limbs of the internal capsules and delayed myelination of the occipital white matter; there is also abnormal, increased signal intensity of the lateral aspects of thalami.

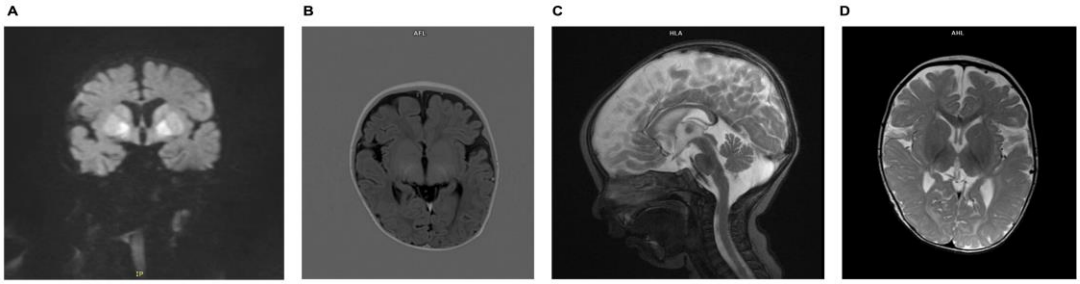

Figure 3. Yeast model for functional validation of variants of uncertain significance (VUS) in *FDXR*. Growth of *Arh1*-null cells transformed with either wild-type *FDXR* (wt), the mutant forms of *FDXR*, or the corresponding empty plasmid (-). p.Arg242Trp is included as a negative control (-) validated by Paul at al., 2017. Yellow numbered boxes indicate the variant severity as demonstrated in the yeast model within a 5-tier system from 1 (most severe) to 5 (least severe).

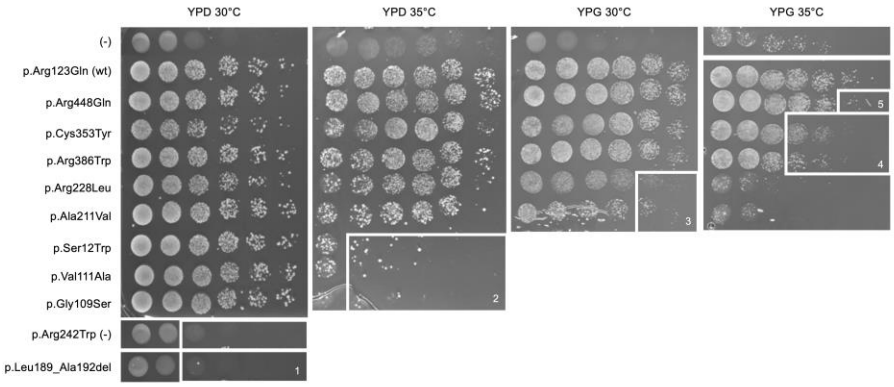

Tables

Table 1. Complete mutation spectrum in *FDXR* of this study as well as all previously published studies.

Variant (NM_024417)	Polypeptide (NP_077728)	Allele frequency (gnomAD)	CADD score	SIFT score	PolyPhen †	ACMG class	Literature
Missense							
c.35C>G	p.Ser12Trp	0.00E+00	23.2	0.04	0.953	VUS	This study
c.151T>C	p.Phe51Leu	0.00E+00	25	0	0.973	VUS	Peng et al., (2017)
c.221C>T	p.Pro74Leu	1.59E-05	25.5	0	1	VUS	Peng et al., (2017)
c.325G>A	p.Gly109Ser	4.00E-06	28.5	0.01	1	VUS	This study
c.332T>C	p.Val111Ala	0.00E+00	26.8	0	0.999	VUS	This study
c.427A>T	p.Ile143Phe	0.00E+00	22.7	0	0.984	VUS	Peng et al., (2017)

c.463C>T	p.Arg155Trp	1.42E-05	24.4	0	1	VUS	Slone et al., (2018)
c.472G>A	p.Val158Met	7.97E-06	26.2	0	0.999	VUS	Peng et al., (2017)
c.578G>A	p.Arg193His	1.61E-05	31	0	0.999	VUS	Slone et al., (2018)
c.613A>G	p.Thr205Ala	0.00E+00	26.5	0	0.989	VUS	Peng et al., (2017)
c.619A>T	p.Ile207Phe	0.00E+00	29.5	0	0.999	VUS	Peng et al., (2017)
c.632C>T	p.Ala211Val	0.00E+00	29.1	0	0.867	VUS	This study
c.643C>G	p.Leu215Val	0.00E+00	31	0	0.999	LP	Paul et al., (2017)
c.683G>T	p.Arg228Leu	1.59E-05	32	0	1	VUS	This study
c.724C>T	p.Arg242Trp	3.19E-05	32	0	1	VUS	Paul et al., (2017)
c.916C>T	p.Arg306Cys	2.89E-05	24.7	0.02	0.959	VUS	Paul et al., (2017)
c.979C>A	p.Arg327Ser	0.00E+00	25.3	0	0.946	VUS	Paul et al., (2017)
c.1058G>A	p.Cys353Tyr	2.12E-05	27.2	0	1	VUS	Peng et al., (2017)
c.1102G>A	p.Asp368Asn	7.96E-06	24.8	0	0.931	VUS	Peng et al., (2017)
c.1156C>T	p.Arg386Trp	1.80E-04	32	0.01	0.999	VUS	Peng et al., (2017)
c.1208C>T	p.Pro403Leu	1.21E-05	27.6	0	1	VUS	Peng et al., (2017)
c.1309G>T	p.Gly437Cys	8.03E-06	25.9	0	1	LP	Peng et al., (2017)
c.1309G>A	p.Gly437Ser	8.03E-06	25.5	0	0.998	VUS	Peng et al., (2017)
c.1343G>A	p.Arg448Gln	8.12E-06	32	0.03	0.926	VUS	This study
c.1429G>A	p.Glu477Lys	0.00E+00	24.7	0	1	VUS	Paul et al., (2017)
Nonsense							
c.820A>T	p.Lys274*	0.00E+00	44			P	Peng et al., (2017)
c.925C>T	p.Arg309*	4.13E-05	41			P	Peng et al., (2017)
c.1255C>T	p.Gln419*	0.00E+00	41			P	Paul et al., (2017)
Indel							
c.576delTCTGGACGTGGC	p.Leu189_Ala192del	4.02E-06				VUS	This study
c.929delG	p.Ser310fs	0.00E+00				VUS	Slone et al., (2018)
Start loss							
c.1A>G	p.Met1?	0.00E+00	21.9			VUS	Slone et al., (2018)

B: benign, US: uncertain significance, LP: likely pathogenic, P: pathogenic

† probability of pathogenicity according to PolyPhen

Table 2. Clinical data of affected individuals in this study

Families	**F1**	**F2**	**F3**		**F4**	**F5**	**F6**
Origin	Germany	Germany	Germany		Poland	France	Hispanic
Subject	**1**	**2**	**3.1**	**3.2**	**4**	**5**	**6**
Gender	F	M	F	M	M	F	F
Genotype †	c.35C>G (p.Ser12Trp) c.683G>T (p.Arg228Leu)	c.332T>C (p.Val111Ala) c.576delTCTGGACGTGGC (p.Leu189_Ala192del)	c.325G>A (p.Gly109Ser) c.1343G>A (p.Arg448Gln)	c.325G>A (p.Gly109Ser) c.1343G>A (p.Arg448Gln)	c.683G>T (p.Arg228Leu) c.1058G>A (p.Cys353Tyr)	c.632C>T (p.Ala211Val) c.632C>T (p.Ala211Val)	c.1156C>T (p.Arg386Trp) c.1156C>T (p.Arg386Trp)
Age at presentation	Childhood	7 months	4 years	4 years	2 months	4 years	5 months
Age last seen	Childhood (alive)	11 months (died)	8 years (alive)	6 years (alive)	17 months (died)	4 years (alive)	4 years (alive)
Hearing impairment	Yes	No	Yes	No	Yes	Yes	No
Optic atrophy	Yes	Yes	No	No	Yes	Yes	Yes
Muscular	Myopathy, hypotonia, ptosis, ophthalmoplegia	Myopathy					Hypotonia
Neurological	Dystonia, ataxia, polyneuropathy	Developmental delay, seizures, nystagmus	Microcephaly, developmental regression, movement disorder, ataxia	Microcephaly, movement disorder, ataxia	Microcephaly, developmental regression, progressive encephalopathy, hypotonia	Developmental regression, spasticity, ataxia	Global developmental delay, developmental regression, non-ambulatory
MRI changes	BGL, BOA	BGL, BOA	Normal	NP	DM, CA	CA, CBA, BOA	BOA
Infection related deterioration	No	Yes	Yes	Yes	No	No	No
Additional phenotypes	Type I diabetes mellitus, psychiatric disorder	Anemia, raised CSF lactate, respiratory insufficiency			Cataract, respiratory distress, feeding difficulties		Retinal dystrophy, strabismus
NPMDS score	14	27	11	3	27	13	19

BGL: basal ganglia lesions, BOA: bilateral optic atrophy, NP: not performed, CA: cerebral atrophy, CBA: cerebellar atrophy, DM: delayed myelination, CSF: cerebrospinal fluid

†Annotation: Transcript (NM_024417) Protein (NP_077728)